Combining the Gap-Tooth Scheme with Projective Integration: Patch Dynamics

CHAPTER · MARCH 2006

DOI: 10.1007/3-540-26444-2_12

3 AUTHORS, INCLUDING:

Giovanni Samaey
University of Leuven
55 PUBLICATIONS **529** CITATIONS

SEE PROFILE

Dirk Roose
University of Leuven
271 PUBLICATIONS **4,030** CITATIONS

SEE PROFILE

Combining the Gap-Tooth Scheme with Projective Integration: Patch Dynamics

Giovanni Samaey[1], Dirk Roose[1], and Ioannis G. Kevrekidis[2]

[1] Department of Computer Science, K.U. Leuven, Celestijnenlaan 200A, 3000 Leuven, Belgium.
{giovanni.samaey,dirk.roose}@cs.kuleuven.ac.be
[2] Department of Chemical Engineering, PACM and Department of Mathematics, Princeton University, Princeton, NJ, USA.
yannis@princeton.edu

Summary. An important class of problems exhibits macroscopically smooth behaviour in space and time, while only a microscopic evolution law is known, which describes effects on fine space and time scales. A simulation of the full microscopic problem in the whole space-time domain can therefore be prohibitively expensive. In the absence of a simplified model, we can approximate the macroscopic behaviour by performing appropriately initialized simulations of the available microscopic model in a number of small spatial domains ("boxes") over a relatively short time interval. Here, we show how to obtain such a scheme, called "patch dynamics," by combining the gap-tooth scheme with projective integration. The gap-tooth scheme approximates the evolution of an unavailable (in closed form) macroscopic equation in a macroscopic domain using simulations of the available microscopic model in a number of small boxes. The projective integration scheme accelerates the simulation of a problem with multiple time scales by taking a number of small steps, followed by a large extrapolation step. We illustrate this approach for a reaction-diffusion homogenization problem, and comment on the accuracy and efficiency of the method.

Key words: equation-free multiscale computation, gap-tooth scheme, patch dynamics, homogenization

1 Introduction

For an important class of multiscale problems, a separation of scales exists between the (microscopic, detailed) level of description of the available model, and the (macroscopic, continuum) level at which one would like to observe the system. Consider, for example, a kinetic Monte Carlo model of bacterial chemotaxis [24]. A stochastic biased random walk model describes the probability of an individual bacterium to run or "tumble," based on the rotation of its flagella. Technically, it would be possible to run the detailed model in the whole space-time domain, and observe the macroscopic variables of interest, but this could be prohibitively expensive. It

is known, however, that, under certain conditions, the evolution of *concentration* of the bacteria as a function of space and time obeys a deterministic evolution law on macroscopic scales sufficiently well; only, in general this evolution law cannot be written down explicitly in closed form.

The recently proposed *equation-free framework* [14, 25] can then be used to confine the use of stochastic time integration to a small fraction of the space-time domain. This framework is built around the central idea of a *coarse time-stepper*, which consists of the following steps: (1) *lifting*, i.e. the creation of *appropriate* initial conditions for the microscopic model, conditioned upon the prescribed initial conditions for the macroscopic (coarse) variables; (2) *evolution*, using the microscopic model and (possibly) some constraints for a time δt; and (3) *restriction*, i.e. the projection of the detailed solution to the macroscopic "observation" variables. This procedure amounts to a time-δt map from coarse variables to coarse variables. This coarse time-stepper can subsequently be used as "input" for time-stepper based algorithms performing macroscopic numerical analysis tasks. These include, for example, time-stepper based bifurcation codes to perform bifurcation analysis for the unavailable macroscopic equation [26, 25, 18, 19]. A coarse time-stepper can also be used in conjunction with a *projective integration method* to increase efficiency of time integration in the presence of time scale separation [6, 7].

When dealing with systems that would be described by (in our case, unavailable) *partial* differential equations, one may also be able to reduce the *spatial* complexity. For systems with one space dimension, the *gap-tooth scheme* [14, 22, 21] was proposed; it can be generalized in several space dimensions. A number of small intervals, separated by large gaps, are introduced; they qualitatively correspond to mesh points for a traditional, continuum solution of the unavailable equation. In higher space dimensions, these intervals would become *boxes* around the coarse mesh points, a term that we will also use throughout this paper. We construct a coarse time-δt map as follows. We first choose a number of macroscopic grid points. Then, we choose a small interval around each grid point; initialize the fine scale, microscopic solver within each interval consistently with the macroscopic initial condition profiles (*lift*); and provide each box with appropriate boundary conditions. Subsequently, we use the microscopic model in each interval to simulate until time δt (*run*), and obtain macroscopic information (*restrict*, e.g. by computing the average density in each box) at time δt. This amounts to a coarse time-δt map.

The gap-tooth scheme was analyzed for pure diffusion [14] and reaction-diffusion homogenization problems [22], where it was shown to be close to a finite difference space discretization for the effective equation, combined with an explicit Euler step in time. For this problem, the "microscopic" model is a partial differential equation with rapidly oscillating coefficients. The macroscopic model is the *effective* equation that describes the evolution of the average behaviour. In the limit, when the period of the oscillations becomes zero, this effective equation is the classical homogenized equation. The goal of the gap-tooth scheme is to approximate the effective equation by using only the microscopic problem inside the small boxes. A related numerical approach to obtain the effective equation was presented in [20]. There, however,

the simulations were performed over the full spatial domain, instead of a number of small boxes.

Generally, a given microscopic code allows us to run with a set of pre-defined boundary conditions. It is highly non-trivial to impose macroscopically inspired boundary conditions on such microscopic codes, see e.g. [17] for a control-based strategy. This can be circumvented by introducing buffer regions at the boundary of each small box, which shield the *short-time* dynamics within the computational domain of interest from boundary effects. One then uses the microscopic code with its *built-in* boundary conditions. The gap-tooth scheme with buffers was introduced in [21, 22]. In this paper, we illustrate the relation between buffer size, time-step and accuracy numerically. More detail will be given in [23].

Since the gap-tooth time-stepper is a time-δt map from coarse variables to coarse variables, we can combine it with projective integration. The resulting scheme is called *patch dynamics* [14]. It advances the macroscopic variables on macroscopic space and time scales, using only simulations in small portions of the space-time domain. To this end, the projective integration scheme takes a few gap-tooth steps of size δt, and extrapolates the obtained macroscopic states using a (large) step size Δt. Here, we will show how to implement these ideas in the context of numerical homogenization. We will use the gap-tooth scheme with buffers as a coarse time-stepper, and combine this with a projective forward Euler step.

In their recent work, inspired by our equation-free approach, E and Engquist and collaborators address the same problem of simulating only the macroscopic behaviour of a multiscale model, see e.g. [3]. In what they call the heterogeneous multiscale method, a macroscale solver is combined with an estimator for quantities that are unknown because the macroscopic equation is not available. This estimator consequently uses appropriately constrained runs of the microscopic model [3]. It should be clear that patch dynamics does exactly this: by taking one gap-tooth step, we estimate the time derivative of the unknown effective equation, and give this as input to an ODE solver, such as projective integration. The elements of the gap-tooth step itself are based on an explicit in time macroscopic finite difference solver (the initial conditions within a box and the boundary conditions for each box are designed based on what a macroscopic finite difference scheme effectively approximates). The difference in their work is that, for conservation laws, the macro-field time derivative is estimated from the *flux* of the conserved quantity; the generalized Godunov scheme is based on this principle. Perhaps the most important difference in implementation, which also affects the numerical analysis, is the fact that we try to minimize changes to a *given microscopic simulator*. In this context, imposing the constraints required by the specific implementation proposed in [3] may be impractical (e.g. if there are constraints on macroscopic quantities that have to be estimated), undesirable (e.g. if the development of the code is expensive and time-consuming) or even impossible (e.g. if the microscopic code is a *legacy code*). Due to the use of buffers such problem are to some extent mitigated in our implementation (at the cost of simulating in larger patches).

Here, we investigate the behaviour of the patch dynamics scheme (with buffers) for a homogenization reaction-diffusion problem. The paper is organized as follows.

In Sect. 2, we formally state the problem that we want to solve. Subsequently, we summarize earlier results on the gap-tooth scheme in Sect. 3, and we describe the full patch dynamics scheme in Sect. 4. We discuss convergence in Sect. 5 and we conclude in Sect. 6.

2 Problem Statement

As a model problem, we consider the following parabolic partial differential equation,

$$\frac{\partial}{\partial t}u_\epsilon(x,t) = \frac{\partial}{\partial x}\left(a\left(\frac{x}{\epsilon}\right)\frac{\partial}{\partial x}u_\epsilon(x,t)\right) + g(u_\epsilon(x,t)), \tag{1}$$

with initial condition $u_\epsilon(x,0) = u^0(x)$ and suitable boundary conditions. In this equation, $a(y) = a\left(\frac{x}{\epsilon}\right)$ is periodic in y and ϵ is a small parameter.

Consider equation (1) with Dirichlet boundary conditions $u_\epsilon(0,t) = v_0$ and $u_\epsilon(1,t) = v_1$. According to classical homogenization theory [1], the solution to (1) can be written as an asymptotic expansion in ϵ,

$$u_\epsilon(x,t) = u_0(x,t) + \sum_{i=1}^{\infty} \epsilon^i u_i(x, \frac{x}{\epsilon}, t), \tag{2}$$

where the functions $u_i(x,y,t) \equiv u_i(x, \frac{x}{\epsilon}, t)$, $i = 1, 2, \ldots$ are periodic in y. Here, $u_0(x,t)$ is the solution of the *homogenized equation*

$$\frac{\partial}{\partial t}u_0(x,t) = \frac{\partial}{\partial x}\left(a^*\frac{\partial}{\partial x}u_0(x,t)\right) + g(u_0(x,t)) \tag{3}$$

with initial condition $u_0(x,0) = u^0(x)$ and Dirichlet boundary conditions $u_0(0,t) = v_0$ and $u_0(1,t) = v_1$; a^* is the constant effective diffusion coefficient, given by

$$a^* = \int_0^1 a(y)\left(1 - \frac{\mathrm{d}}{\mathrm{d}y}\chi(y)\right)\mathrm{d}y, \tag{4}$$

and $\chi(y)$ is the periodic solution of

$$\frac{\mathrm{d}}{\mathrm{d}y}\left(a(y)\frac{\mathrm{d}}{\mathrm{d}y}\chi(y)\right) = \frac{\mathrm{d}}{\mathrm{d}y}a(y), \tag{5}$$

the so-called *cell problem*. The solution of (5) is only defined up to an additive constant, so we impose the extra condition

$$\int_0^1 \chi(y)\mathrm{d}y = 0. \tag{6}$$

From this cell problem, we can derive $u_1(x,y,t) = \frac{\partial u_0}{\partial x}\chi(y)$.

These asymptotic expansions have been rigorously justified in the classical book [1]. Under appropriate smoothness assumptions, one can obtain pointwise convergence of u_ϵ to u_0 as $\epsilon \to 0$. Therefore, we can write

$$\|u_\epsilon(x,t) - u_0(x,t)\| \leq C_0\epsilon, \tag{7}$$

where $\|f(x)\| \equiv \|f(x)\|_\infty = \max_x |f(x)|$ denotes the ∞-norm of f. Throughout this text, whenever we use $\|\cdot\|$, we mean the ∞-norm.

For $u(x,t)$ sufficiently smooth, the averaged function

$$U(x,t) = \mathcal{S}_h(u)(x,t) := \frac{1}{h}\int_{x-\frac{h}{2}}^{x+\frac{h}{2}} u(\xi,t)\mathrm{d}\xi$$

can be asymptotically expanded in h as follows,

$$U(x,t) = u(x,t) + \sum_{l=1}^{\infty}\left(\frac{h}{2}\right)^{2l}\frac{1}{(2l+1)!}\frac{\partial^{2l}}{\partial^{2l}\xi}u(\xi,t)\bigg|_{\xi=x}.$$

The difference between the homogenized solution $u_0(x,t)$ and the averaged solution $U(x,t) = h^{-1}\int_{x-\frac{h}{2}}^{x+\frac{h}{2}} u_\epsilon(\xi,t)\mathrm{d}\xi$ is bounded by

$$\|U(x,t) - u_0(x,t)\| \leq C_1h^2 + C_2\epsilon.$$

Therefore, the averaged solution is a good approximation of the homogenized solution for sufficiently small box width h.

The goal of the gap-tooth scheme is to approximate the solution $U(x,t)$, while only making use of the detailed model (1). Moreover, we assume that a time integration code for (1) has already been written and is available with a number of *standard* boundary conditions, such as no-flux or Dirichlet.

3 The Gap-Tooth Scheme

We briefly revise the gap-tooth algorithm as it was introduced in [21, 22]. Suppose we want to obtain the solution of the *unknown* equation (3) on the interval $[0,1]$, using an equidistant, macroscopic mesh $\mathit{\Pi}(\Delta x) := \{0 = x_0 < x_1 = x_0 + \Delta x < \ldots < x_N = 1\}$. To this end, consider a small interval (*tooth*, "inner" box) of length $h \ll \Delta x$ centered around each mesh point, as well as an interval of size $H > h$ (the *buffer* box). (See Fig. 1.) To perform time integration using the microscopic model (1) in each box, we provide each box with initial and boundary conditions as follows.

Initial Condition

We define the initial condition by constructing a polynomial, based on the (given) box averages U_i^n, $i = 1, \ldots, N$,

$$\tilde{u}^i(x,t_n) \approx p_i^d(x;t_n), \qquad x \in [x_i - \frac{H}{2}, x_i + \frac{H}{2}], \tag{8}$$

where $p_i^d(x;t_n)$ denotes a polynomial of (even) degree d, and H denotes the size of the buffer. We require that the approximating polynomial has the same box averages as the initial condition in box i and in $\frac{d}{2}$ boxes to the left and to the right. This gives us

$$\frac{1}{h}\int_{x_{i+j}-\frac{h}{2}}^{x_{i+j}+\frac{h}{2}} p_i^d(\xi;t_n)\mathrm{d}\xi = U_{i+j}^n, \qquad j = -\frac{d}{2},\ldots,\frac{d}{2}. \tag{9}$$

The box averages are computed over the inner box of width h. One can easily check that

$$\mathcal{S}_h(p_i^d)(x,t_n) = \sum_{j=-\frac{d}{2}}^{\frac{d}{2}} U_{i+j}^n L_{i,j}^d(x), \qquad L_{i,j}^d(x) = \prod_{\substack{l=-\frac{d}{2} \\ l\neq j}}^{\frac{d}{2}} \frac{(x - x_{i+l})}{(x_{i+j} - x_{i+l})} \tag{10}$$

where $L_{i,j}^d(x)$ denotes a Lagrange polynomial of degree d.

Boundary Conditions

The time integration of the microscopic model in each box should provide information on the evolution of the global problem at that location in space. It is therefore crucial that the boundary conditions are chosen such that the solution inside each box evolves *as if it were embedded in a larger domain*. We already mentioned that, in many cases, it is not possible or convenient to impose macroscopically-inspired constraints on the microscopic model (e.g. as boundary conditions). However, we can introduce a larger box of size $H \gg h$ around each macroscopic mesh point, but still only use (for macro-purposes) the evolution over the smaller, inner box. The simulation can subsequently be performed using any of the *built-in* boundary conditions of the microscopic code. Lifting and evolution (using *arbitrary* available boundary conditions) are performed in the larger box; yet the restriction is done by processing the solution (here taking its average) over the inner, small box only. The goal of the additional computational domains, the *buffers*, is to buffer the solution inside the small box from the artificial disturbance caused by the boundary conditions. This can be accomplished over *short enough* times, provided the buffers are *large enough*; analyzing the method is tantamount to making these statements quantitative.

The idea of using a buffer region was also used in the multiscale finite element method (oversampling) of Hou [12] to eliminate the boundary layer effect; also Hadjiconstantinou makes use of overlap regions to couple a particle simulator with a continuum code [11]. If the microscopic code allows a choice of different types of microscopic boundary conditions, selecting the size of the buffer may also depend on this choice.

The Algorithm

The complete *gap-tooth* algorithm to proceed from t_n to $t_{n+1} = t_n + \delta t$ is given below:

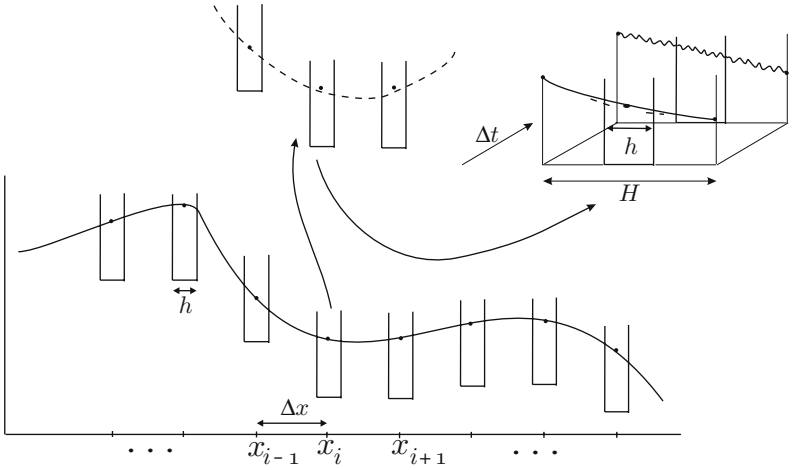

Fig. 1. A schematic representation of a gap-tooth time step with buffer boxes. We choose a number of boxes of size h around each macroscopic mesh point x_i and interpolate the initial averages (dots) in a number of boxes around x_i. This polynomial is taken as the initial condition around x_i, and simulation is performed in boxes of size H

1. At time t_n, construct the initial condition $\tilde{u}^i(x, t_n)$, $i = 0, \ldots, N$, using the box averages U_j^n ($j = 0, \ldots, N$), as defined in (8-9).
2. Compute $\tilde{u}^i(x, t)$ by solving the equation (1) in the interval $[x_i - \frac{H}{2}, x_i + \frac{H}{2}]$ until time $t_{n+1} = t + \delta t$ with *some* boundary conditions. The boundary conditions can be anything that the time integration routine allows.
3. Compute the box average U_i^{n+1} at time t_{n+1}.

It is clear that this amounts to a map of the macroscopic variables $U^n \approx U(n\delta t)$ at time t_n, to the macroscopic variables U^{n+1} at time $t_{n+1} = t_n + \delta t$, i. e. a "coarse to coarse" time-δt map. We write this map as follows,

$$U^{n+1} = S_d(U^n; t_n + \delta t), \tag{11}$$

where S represents the numerical time-stepping scheme for the macroscopic (coarse) variables and d denotes the degree of the interpolating polynomial. Here, $U(t)$ is the exact solution of a system of ordinary differential equations that represent a method of lines semi-discretization of the effective equation, while $U^n \approx U(n\delta t)$ represents a numerical approximation to this solution.

Microscopic Simulators

Above, we have assumed that the microscopic model is a partial differential equation. However, some microscopic simulators are of a different nature, e.g. kinetic Monte Carlo or molecular dynamics codes. In fact, this is the case where we expect our method to be most useful. In this case, several complications arise. First of all, the choice of the box width h becomes important, since there will generally exist

a trade-off between statistical accuracy (e.g. enough sampled particles) and spatial resolution.

Second, the *lifting* step, i.e. the construction of box initial conditions, also becomes more involved. In general, the microscopic model will have many more degrees of freedom, the *higher order moments* of the evolving distribution. These will quickly become slaved to the governing moments (the ones where the lifting is conditioned upon), see e.g. [14, 18], but it might be better to do a "constrained" run before initialization to create "mature" initial conditions [13, 8, 15, 4, 2].

Finally, determining which and how many neighbouring boxes are needed for the interpolation polynomial is a delicate issue. The degree of the interpolation polynomial determines how many spatial derivatives are initialized consistently in each box. This is related with the order of the partial differential equation, i.e. the order of the highest spatial derivative. A systematic way to estimate this order, without having the macroscopic equation, is given in [16].

Numerical experiments with the gap-tooth scheme using a kinetic Monte Carlo microscopic model are presented in [10, 5].

4 Patch Dynamics

Once we have constructed a coarse time-stepper that exploits the *spatial* scale separation, we can combine it with the projective integration scheme [6] to exploit *time* scale separation. The crucial idea is that one can estimate the time derivative of the macroscopic system using the gap-tooth scheme, and perform a large extrapolation step.

We will briefly summarize the projective integration scheme as it was presented in [14, 6], and subsequently show how to combine it with the gap-tooth scheme.

The Projective Integration Scheme

Let $\Delta t \gg \delta t$ be a large time step (commensurate with the slow dynamics), and denote the numerical approximations of the coarse solution $U(t)$ as $U^n \approx U(n\Delta t)$. Suppose we are given a (coarse) time-stepper that permits to compute

$$U^{\alpha,n} = S(U^{0,n}, t_n + \alpha\delta t), \tag{12}$$

for $\alpha \in [0, 1]$. Here, $U^{\alpha,n} \approx U(n\Delta t + \alpha\delta t)$, and therefore we have $U^{0,n} = U^n$ by consistency.

We cannot afford to compute $U^{n+1} \approx U((n+1)\Delta t)$ this way, because $\Delta t \gg \delta t$. Instead, we compute U^{n+1} by extrapolation, using a coarse *projective* scheme of the type

$$U^{n+1} = U^{\alpha,n} + (\Delta t - \alpha\delta t)\tilde{F}(U^{k,n}), \tag{13}$$

where we approximate the time derivative by

$$\tilde{F}(U^{\alpha,n}) = \frac{U^{1,n} - U^{\alpha,n}}{(1-\alpha)\delta t} \tag{14}$$

for some α in $[0, 1)$, which has to be chosen large enough to ensure that lifting errors have been removed by the microscopic simulation. (The higher order moments are then slaved to the lower order ones.) Here, assuming that lifting errors can be neglected, we choose $\alpha = 0$. As discussed in Sect. 3, techniques to minimize lifting errors can be devised, and therefore the choice $\alpha = 0$ is not that artificial. The time step Δt has to be chosen such that the resulting macroscopic time-stepper is stable. In order to increase the stability region, one could take $k > 1$ gap-tooth steps before performing the extrapolation, see [14, 9] for more details.

Patch Dynamics for the Homogenization Problem

It is clear that the gap-tooth time-stepper, constructed in Sect. 3, can be considered as a coarse time-stepper for the projective integration scheme. Here, for simplicity, we take one gap-tooth step with $\alpha = 0$ for the projective integration. (Taking $k > 1$ gap-tooth steps might lead to an increased stability region [6].) This gives the following algorithm (Fig. 2).

1. At time t_n, take *one* gap-tooth step,
$$U^{1,n} = S_d(U^n, t_n + \delta t)$$
2. Compute the approximate effective time derivative as
$$\tilde{F}(U^n) = \frac{U^{1,n} - U^{0,n}}{\delta t}$$
3. Perform a projective forward Euler step, using this approximate time derivative.
$$U^{n+1} = U^n + \Delta t \tilde{F}(U^n)$$

5 Convergence Results

Theoretical Results

We can easily obtain a convergence result for patch dynamics taking advantage of a theorem from [3].

If we would have the macroscopic equation (3), we could obtain a method of lines semi-discretization by replacing the spatial derivatives by finite differences of order d, yielding a system of ordinary differential equations of the form

$$\dot{U} = F(U). \tag{15}$$

Consider as a macroscopic solver a standard forward Euler scheme

$$U^{n+1} = U^n + \Delta t F(U^n). \tag{16}$$

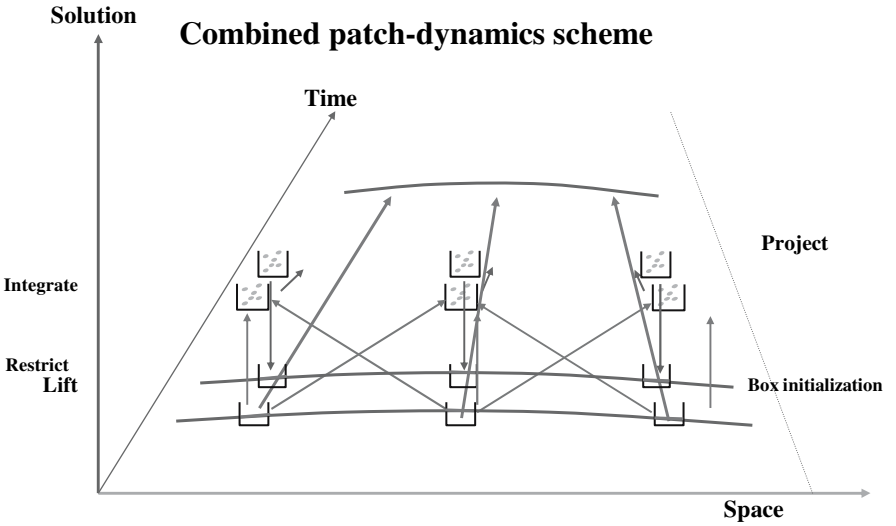

Fig. 2. A schematic representation of a patch dynamics scheme. After a gap-tooth step, we extrapolate over a large time step

Because the macroscopic equation is not available, we need to estimate $F(U^n)$, by taking a gap-tooth step,

$$U^{n+1} = U^n + \Delta t \tilde{F}(U^n), \qquad \tilde{F}(U^n) = \frac{U^{1,n} - U^{0,n}}{\delta t}. \tag{17}$$

Then, under appropriate assumptions on F and U, we can state that [3]

Theorem 1. *Patch dynamics is stable if the forward Euler scheme is stable. Moreover, the total discretization error is bounded by*

$$\|U^n - U(t_n)\| \leq C(\Delta t + \max_{0 \leq k \leq \frac{t_n}{\Delta t}} \|F(U^k) - \tilde{F}(U^k)\|),$$

where $U(t_n)$ is the exact solution of the semi-discrete system (15).

Thus, what remains is to estimate $\|F(U^k) - \tilde{F}(U^k)\|$. We mention a theorem that shows the error that is made in the estimation of the time derivative.

Theorem 2. *Consider the model problem (1). When performing one gap-tooth step with Dirichlet boundary conditions,*

$$U^{1,n} = S_d(U^n, t_n + \delta t),$$

we can bound the error

$$\|\tilde{F}(U^n) - F(U^n)\| \leq C\left(h^2 + \frac{\epsilon}{\delta t} + \delta t^2 + E(\delta t, H)\right), \tag{18}$$

where $F(U^n)$ is the time derivative as defined by (15) for (3) and

$$\lim_{H\to\infty} E(\delta t, H) = \lim_{\delta t\to 0} E(\delta t, H) = 0$$

In this theorem, $E(\delta t, H)$ represents the error term that is due to the buffers. We see that this term can be made arbitrarily small by choosing H large enough and δt small enough. A heuristic to make this error term comparable in size with the others is given in [23], where this theorem is proved. Also, due to the term $\frac{\epsilon}{\delta t}$, it is impossible to obtain convergence when the small scale ϵ is fixed. In this context, the theorem has to be seen as a bound for optimal error.

Numerical Results

Consider the following model problem,

$$\frac{\partial}{\partial t}u_\epsilon(x,t) = \frac{\partial}{\partial x}\left(a(\frac{x}{\epsilon})\frac{\partial}{\partial x}u_\epsilon(x,t)\right), \qquad a(\frac{x}{\epsilon}) = 1.1 + \sin(2\pi\frac{x}{\epsilon}) \tag{19}$$

with $\epsilon = 1\cdot 10^{-5}$, $x\in[0,1]$, initial conditions $u_\epsilon(x,0) = 1-4(x-0.5)^2$, and Dirichlet boundary conditions $u_\epsilon(0,t) = u_\epsilon(1,t) = 0$. We choose $\epsilon = 1\cdot 10^{-5}$. To solve the microscopic problem, we use a standard finite difference discretization in space and a variable step/variable order time integration method (`ode23s` in Matlab), with mesh width $\delta x = 1\cdot 10^{-7}$. The corresponding homogenized equation is given by

$$\frac{\partial}{\partial x}\left(a^*\frac{\partial}{\partial x}u_0(x,t)\right), \qquad a^* \approx 0.45825686. \tag{20}$$

We first investigate the error in the time derivative estimator (18) as a function of buffer size and time step. To this end, we take a gap-tooth step with $\Delta x = 0.1$ and $h = 2\cdot 10^{-3}$. We let the buffer size H vary from $2\cdot 10^{-3}$ to $3\cdot 10^{-2}$, and the time step from $1\cdot 10^{-7}$ to $5\cdot 10^{-6}$. Inside each box, we use the microscopic solver with Dirichlet boundary conditions. For the lifting step, we use quadratic interpolation, which is equivalent to a standard second order finite difference approximation of the diffusion term [22]. Figure 3 shows the evolution of the error as a function of buffer width and time step. The error is measured as the difference of (18) with respect to the second order finite difference discretization of the homogenized equation (3),

$$F(U_j^n) = a^*\frac{U_{j+1}^n - 2U_j^n + U_{j-1}^n}{\Delta x^2}$$

The leftmost picture shows the error as a function of buffer size for a fixed time step. We see that the error decreases exponentially with the buffer size. We see that the smaller the time step, the faster the initial decay of the error, but the optimal error that can be obtained is larger. This is due to the term $\frac{\epsilon}{\delta t}$ in (18). This is made clear in the rightmost picture, which shows the error as a function of time step, for a fixed buffer size. We expect that for a fixed buffer size, the error decreases with decreasing time step, and the optimal error curve has a slope $\frac{1}{\delta t}$. This is visible only for very small δt, due to interference with the time integration error of the microscopic solver.

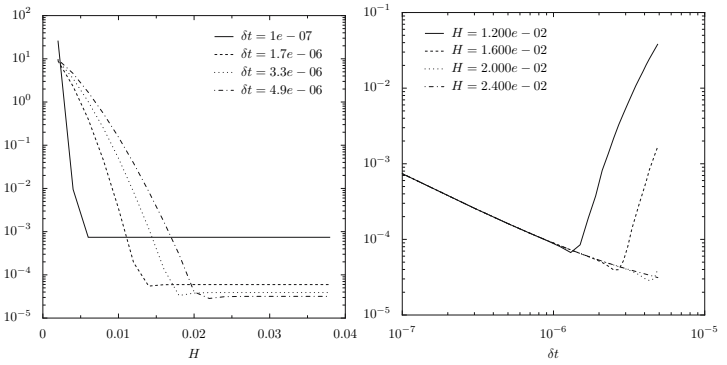

Fig. 3. Left: Error of gap-tooth time derivative estimate in function of buffer size for the given values of the time step δt. Right: Error of gap-tooth time derivative estimate in function of time step for the given values of the buffer size

In order to show the convergence in the absence of this term, we performed the same experiment, but we replaced the microscopic solver with a finite difference discretization of the homogenized equation. The result is shown in Fig. 4. We see that we have convergence up to 8 digits. The remaining digits are lost due to cancellation errors in estimating the derivative.

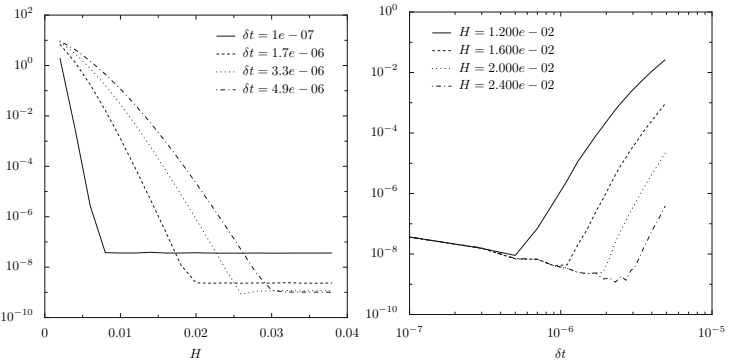

Fig. 4. Left: Error of gap-tooth time derivative estimate in function of buffer size for a the give values of the time step δt, using the homogenized equation as a microscopic solver. Right: Error of gap-tooth time derivative estimate in function of time step for the given value of the buffer size H

Next, we use patch dynamics to integrate this system until $t = 1$. We choose $\Delta t = 1 \cdot 10^{-3}$. In this case $\nu = \frac{\Delta t}{\Delta x^2} = 0.1$, so the macroscopic scheme is certainly stable. Based on the previous tests, we choose a buffer size of $H = 7 \cdot 10^{-3}$ and $\delta t = 1 \cdot 10^{-6}$. Figure 5 shows the results. We depict the error with respect to the finite difference scheme on the homogenized equation in the accompanying table.

We see that the scheme has the ability of computing the solution to the unavailable homogenized equation with 3 correct digits, using simulations on only 7% of the spatial domain and 0.1% of the time domain (a gap-tooth time step of 10^{-6} versus a macroscopic time step of 10^{-3}).

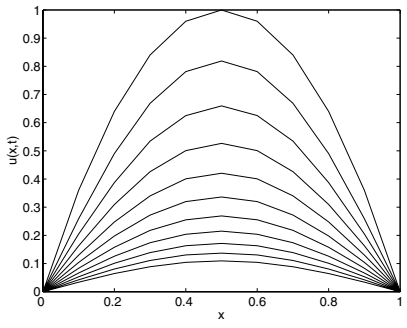

time	error
$5 \cdot 10^{-2}$	$6.4683 \cdot 10^{-4}$
$1 \cdot 10^{-1}$	$1.9202 \cdot 10^{-3}$
$1.5 \cdot 10^{-1}$	$8.3803 \cdot 10^{-4}$
$2 \cdot 10^{-1}$	$1.2133 \cdot 10^{-3}$
$2.5 \cdot 10^{-1}$	$9.8365 \cdot 10^{-4}$
$3 \cdot 10^{-1}$	$1.2383 \cdot 10^{-3}$
$3.5 \cdot 10^{-1}$	$1.0178 \cdot 10^{-3}$
$4 \cdot 10^{-1}$	$7.4551 \cdot 10^{-4}$
$4.5 \cdot 10^{-1}$	$7.5973 \cdot 10^{-4}$
$5 \cdot 10^{-1}$	$5.6377 \cdot 10^{-4}$

Fig. 5. Left: Solution of the unavailable homogenized equation using patch dynamics, at $t = 0, 5 \cdot 10^{-2}, 1 \cdot 10^{-1}, 1.5 \cdot 10^{-1} \ldots, 5 \cdot 10^{-1}$. Right: Error in maximum norm with respect to the finite difference comparison scheme for the homogenized equation

6 Conclusions

We described a patch dynamics algorithm for the numerical simulation of multi-scale problems. This scheme simulates the macroscopic behaviour over a macroscopic domain when only a microscopic model is explicitly available; it only uses appropriately initialized short simulations over small sub-domains. We numerically illustrated convergence properties of this scheme for a parabolic homogenization problem, and related these properties to theoretical results that were obtained in [3].

We showed that our method approximates a finite difference scheme for the homogenized equation when the buffer regions are chosen large enough with respect to the gap-tooth time step. Our analysis revealed that the presence of microscopic scales introduces errors that can be made small, but not arbitrarily small. In this sense, there is an optimal accuracy that can be reached with these methods.

Numerical simulations on a model problem show that it is possible to obtain simulation results over large space-time domains, using only a fraction of the computational complexity that would be needed by a full microscopic simulation.

Acknowledgments

GS is a Research Assistant for the Fund of Scientific Research – Flanders. This work has been partially supported by grant IUAP/V/22 (Belgian Federal Science Policy

Office) and by the FWO grant G.0130.03 (GS, DR), and an NSF/ITR grant and DOE (IGK).

References

1. A. Bensoussan, J. L. Lions, and G. Papanicolaou. *Asymptotic analysis of periodic structures*, volume 5 of *Studies in Mathematics and its Applications*. North-Holland, Amsterdam, 1978.
2. W. E. Analysis of the heterogeneous multiscale method for ordinary differential equations. *Comm. Math. Sci.*, 1(3):423–436, 2003.
3. W. E and B. Engquist. The heterogeneous multi-scale methods. *Comm. Math. Sci.*, 1(1):87–132, 2003.
4. I. Fatkullin and E. Vanden Eijnden. A computational strategy for multiscale chaotic systems with applications to Lorenz 96 model. 2004. Preprint.
5. C. W. Gear and I. G. Kevrekidis. Boundary processing for Monte Carlo simulations in the gap-tooth scheme. Technical Report 2002-031N, NEC Research Institute, 2002.
6. C. W. Gear and I. G. Kevrekidis. Projective methods for stiff differential equations: problems with gaps in their eigenvalue spectrum. *SIAM Journal of Scientific Computation*, 24(4):1091–1106, 2003. Can be obtained as NEC Report 2001-029, `http://www.neci.nj.nec.com/homepages/cwg/projective.pdf`.
7. C. W. Gear and I. G. Kevrekidis. Telescopic projective methods for stiff differential equations. *Journal of Computational Physics*, 187(1):95–109, 2003.
8. C. W. Gear and I. G. Kevrekidis. Constraint-defined manifolds: a legacy code approach to low-dimensional computation. *J. Sci. Comp.*, 2004. in press.
9. C. W. Gear, I. G. Kevrekidis, and C. Theodoropoulos. "Coarse" integration/bifurcation analysis via microscopic simulators: micro-Galerkin methods. *Computers and Chemical Engineering*, 26(7-8):941–963, 2002.
10. C. W. Gear, J. Li, and I. G. Kevrekidis. The gap-tooth method in particle simulations. *Physics Letters A*, 316:190–195, 2003. Can be obtained as physics/0303010 at `arxiv.org`.
11. N. G. Hadjiconstantinou. Hybrid atomistic-continuum formulations and the moving contact-line problem. *Journal of Computational Physics*, 154:245–265, 1999.
12. T. Y. Hou and X. H. Wu. A multiscale finite element method for elliptic problems in composite materials and porous media. *Journal of Computational Physics*, 134:169–189, 1997.
13. G. Hummer and I. G. Kevrekidis. Coarse molecular dynamics of a peptide fragment: free energy, kinetics and long-time dynamics computations. *Journal of Chemical Physics*, 118(23):10762–10773, 2003. Can be obtained as physics/0212108 at `arxiv.org`.
14. I. G. Kevrekidis, C. W. Gear, J. M. Hyman, P. G. Kevrekidis, O. Runborg, and C. Theodoropoulos. Equation-free multiscale computation: enabling microscopic simulators to perform system-level tasks. *Comm. Math. Sciences*, 1(4):715–762, 2003.
15. I. G. Kevrekidis, C. W. Gear, T. Kaper and A. Zagaris. Projecting to a slow manifold: singularly perturbed systems and legacy codes. submitted, 2004.
16. J. Li, P. G. Kevrekidis, C. W. Gear, and I. G. Kevrekidis. Deciding the nature of the "coarse equation" through microscopic simulations: the baby-bathwater scheme. *SIAM Multiscale modeling and simulation*, 1(3):391–407, 2003.
17. J. Li, D. Liao, and S. Yip. Imposing field boundary conditions in MD simulation of fluids: optimal particle controller and buffer zone feedback. *Mat. Res. Soc. Symp. Proc*, 538:473–478, 1998.

18. A. G. Makeev, D. Maroudas, and I. G. Kevrekidis. Coarse stability and bifurcation analysis using stochastic simulators: kinetic Monte Carlo examples. *Journal of Chemical Physics*, 116:10083–10091, 2002.
19. A. G. Makeev, D. Maroudas, A. Z. Panagiotopoulos, and I. G. Kevrekidis. Coarse bifurcation analysis of kinetic Monte Carlo simulations: a lattice-gas model with lateral interactions. *Journal of Chemical Physics*, 117(18):8229–8240, 2002.
20. O. Runborg, C. Theodoropoulos, and I. G. Kevrekidis. Effective bifurcation analysis: a time-stepper based approach. *Nonlinearity*, 15:491–511, 2002.
21. G. Samaey, I. G. Kevrekidis, and D. Roose. Damping factors for the gap-tooth scheme. In S. Attinger and P. Koumoutsakos, editors, *Multiscale modelling and simulation*, volume 39 of *Lecture Notes in Computational Science and Engineering*, pages 94–103. Springer, 2004.
22. G. Samaey, D. Roose, and I. G. Kevrekidis. The gap-tooth scheme for homogenization problems. *SIAM Multiscale modelling and simulation*, 2005. In press. Can be obtained as physics/03120004 at `arxiv.org`.
23. G. Samaey, I.G. Kevrekidis and D. Roose. Patch dynamics with buffers for homogenization problems. Submitted to *Journal of Computational Physics*, 2004. Can be obtained as physics/0412005 at `arxiv.org`.
24. S. Setayeshar, C. W. Gear, H. G. Othmer, and I. G. Kevrekidis. Application of coarse integration to bacterial chemotaxis. *SIAM Multiscale modelling and simulation*, 2004. In press. Can be obtained as physics/0308040 at `arxiv.org`.
25. C. Theodoropoulos, Y. H. Qian, and I. G. Kevrekidis. Coarse stability and bifurcation analysis using time-steppers: a reaction-diffusion example. In *Proc. Natl. Acad. Sci.*, volume 97, pages 9840–9843, 2000.
26. C. Theodoropoulos, K. Sankaranarayanan, S. Sundaresan, and I. G. Kevrekidis. Coarse bifurcation studies of bubble flow Lattice–Boltzmann simulations. *Chem. Eng. Sci.*, 2004. in press. Can be obtained as nlin.PS/0111040 from `arxiv.org`.